ACCSCIENCE PUBLISHING

International Journal of Bioprinting

CASE STUDY

Customized 3D-printed prosthesis for reconstruction of complex bilateral traumatic knee bone defects: A case report

Gang Zhao[1], Yongqiang Zhang[1], Longfei Liu[1], Longxin An[2], Futian Zhang[1], Da Huo[1], Xuecheng Sun[1], Xiaoming Yang[1]*, and Naibo Feng[1]*

[1]Department of Trauma Orthopedics, Weifang People's Hospital, Shandong Second Medical University, Weifang, Shandong, China

[2]Clinical Medical College, Shandong Second Medical University, Weifang, Shandong, China

(This article belongs to the *Special Issue*: *Multifunctional Bioprinting for Tissue/Organ Engineering*)

Abstract

Composite knee tissue defects involving bone, meniscus, and ligaments caused by high-energy trauma are rare and present significant reconstructive challenges. Herein, we report a case of a 50-year-old woman with bilateral asymmetric knee injuries arising from a traffic accident, including right medial femoral condyle loss with medial collateral ligament (MCL) deficiency, and complex defect involving left-sided bone, meniscus, and MCL, accompanied by degloving injury involving 20% total body surface area. Treatment was performed in the following three stages: debridement, soft tissue coverage, and final reconstruction using data-driven mirror modeling to design patient-specific 3D-printed titanium implants. The right MCL was reconstructed using a LARS artificial ligament. At 12-month follow-up, stable bone–implant integration, flap viability, and functional recovery were observed, with knee flexion of 120° (left) and 80° (right), and Knee Society Scores of 65 and 70. This case highlights the feasibility of personalized 3D-printed implants in complex bilateral knee reconstruction.

Keywords: 3D printing; Knee bone defect; LARS ligament; Medial collateral ligament; Perforator flap

***Corresponding authors:**
Xiaoming Yang
(fristxinmeng@126.com)

Naibo Feng
(Fengnaibo@sdsmu.edu.cn)

Citation: Zhao G, Zhang Y, Liu L, *et al*. Customized 3D-printed prosthesis for reconstruction of complex bilateral traumatic knee defects: A case report. *Int J Bioprint*. 2025;11(5):451-459. doi: 10.36922/IJB025290292

Received: July 17, 2025
Revised: August 7, 2025
Accepted: August 8, 2025
Published Online: August 8, 2025

1. Background

Composite tissue defects of the knee involving the skin, bone, and ligaments represent a severe form of injury that can result in permanent lower limb dysfunction. The management of such injuries remains a significant challenge for orthopedic surgeons. Arthrodesis can address irreparable instability, inadequate soft tissue coverage, and recurrent failure following multiple revisions of joint arthroplasty.[1,2] However, in cases with extensive bone loss at the distal femur and/or proximal tibia, acute limb shortening and compromised vascular integrity caused by altered anatomical alignment may severely impact the patient's quality of life. Therefore, more advanced reconstructive strategies are required to manage these complex injuries.[3]

In the present case, the patient sustained large bilateral knee defects involving both osseous and soft tissue structures. We developed an innovative treatment strategy leveraging recent advancements in 3D printing technology. Using computer modeling and data-driven design, we fabricated customized titanium implants even in the absence of complete CT imaging, and simultaneously reconstructed the medial collateral ligament (MCL) using a LARS synthetic ligament. This approach aimed to restore anatomical integrity, improve functional outcomes, and enhance long-term durability. This case provides new insights into personalized orthopedic solutions for managing complex open knee injuries with extensive bone defect.

2. Case presentation

A 50-year-old female sustained bilateral open knee bone defects accompanied by hemorrhagic shock after being dragged by a motor vehicle during a traffic accident. Radiographic examination revealed a partial defect of the right medial femoral condyle measuring 3.2 × 2.8 cm^2, and a full-thickness defect of the left tibial plateau and femoral condyle measuring 4.5 × 3.6 cm^2. The total area of skin avulsion reached approximately 20% of the body surface area. The patient had no significant past medical history.

On physical examination, the left lower limb showed extensive injury. The anterior knee presented with lacerations, while large areas of skin were lost from the anterior and medial thigh, medial knee, and medial lower leg, involving approximately 4% of the total body surface area. Partial muscle loss was observed in the distal portions of the vastus medialis, hamstrings, and sartorius. There was extensive osseoligamentous loss, affecting the medial femoral condyle, medial tibial plateau, and medial collateral ligament. Distal perfusion was preserved. Additional skin defects were noted at the medial heel and the medial aspect of the first metatarsophalangeal joint (Figure 1A–D). On the right side, there was approximately 3% skin loss involving the medial knee and anterior thigh. The distal vastus medialis was partially missing, and the bone defect involved the medial femoral condyle with associated loss of the medial collateral ligament (Figure 1E). Vascular supply to the distal limb remained intact. Bilateral radiographs confirmed bone defects of both knees (Figure 1F).

2.1. Stage 1: Emergency radical debridement

Under general anesthesia with endotracheal intubation, the patient underwent thorough wound exploration and radical debridement. A "carpet rolling" technique was utilized to remove all contaminated and necrotic soft tissue, as well as devitalized bone fragments, preparing the wounds for subsequent flap coverage and prosthetic reconstruction. Intraoperative findings on the left side revealed complete loss of the medial femoral condyle and medial tibial plateau, while both the anterior and posterior cruciate ligaments remained intact (Figure 2A). On the right side, there was a partial defect of the medial femoral condyle involving the articular surface, along with the absence of the medial collateral ligament (Figure 2B). Following debridement, the wounds were covered with VAC® polyurethane foam dressings (Figure 2C and D).

Once the patient's condition stabilized, a second debridement was performed to remove necrotic subcutaneous tissue and contaminated bone. The bone defects were temporarily filled with polymethyl methacrylate (PMMA) cement, and local skin was mobilized to reduce wound dimensions and minimize exudate (Figure 2E and F). The left lower limb was additionally stabilized with an external fixation brace (Figure 2E). VAC® dressings were reapplied to maintain wound management.

2.2. Stage 2: Flap coverage of the wounds

After emergency debridement and stabilization, early flap coverage was initiated. A 22 × 14 cm^2 left deep inferior epigastric perforator (DIEP) flap was used to cover the right medial knee defect (Figure 3A–C). Microvascular anastomosis was performed between the deep inferior epigastric vessels and the descending branch of the lateral circumflex femoral artery and veins. Sensory nerve coaptation involved intercostal nerve branches and branches of the lateral femoral cutaneous or femoral nerve (Figure 3D).

One week later, after flap stabilization, a 30 × 10 cm^2 latissimus dorsi musculocutaneous flap was used to cover the left knee defect (Figure 3E–G). Anastomosis was performed between the thoracodorsal vessels and the same recipient vessels, with sensory coaptation between thoracodorsal nerve branches and femoral cutaneous nerves. Both flaps survived without complications. Throughout the treatment course, physical therapists guided early mobilization and rehabilitation (Figure 3H and I).

2.3. Stage 3: 3D-printed prosthesis design, implantation, and knee function reconstruction

The third stage involved reconstructing the knee bone defects using data-driven modeling to restore the right medial femoral condyle (Figure 4A–E; Video S1). The left femoral condyle and tibial plateau were reconstructed by

Figure 1. External wounds and radiographic evidence of bone defects. (A–D) Traumatic injuries of the patient's left lower limb, showing extensive soft tissue and skin loss around the knee, thigh, and lower leg. (E) Soft tissue defect over the medial aspect of the right knee and anterior thigh. (F) X-ray images showing bone defects of both knees.

mirroring the anatomy of the reconstructed right knee (Figure 4F–N). A dual-tunnel channel was designed on the tibial side for MCL reconstruction using a LARS synthetic ligament (Figure 4J; Video S2). The 3D-printed prostheses were implanted 6 weeks after flap repair. During this interval, we closely monitored complete blood count, C-reactive protein, and erythrocyte sedimentation rate, proceeding with surgery once all infection-related markers normalized. Postoperative radiographs confirmed accurate prosthesis placement (Figure 5A–D) and proper restoration of lower limb alignment (Figure 5E).

2.4. Follow-up

At the 3-month follow-up, there were no signs of infection or flap necrosis. The patient walked independently with a near-normal range of motion in the right knee. The left knee showed limited flexion but preserved extension (Figure 6A–F). He could walk over 500 m unaided with minimal pain (VAS score: 1/10; Video S3). By 12 months postoperatively, the patient could already walk almost normally, with only a slight limp (Video S4).

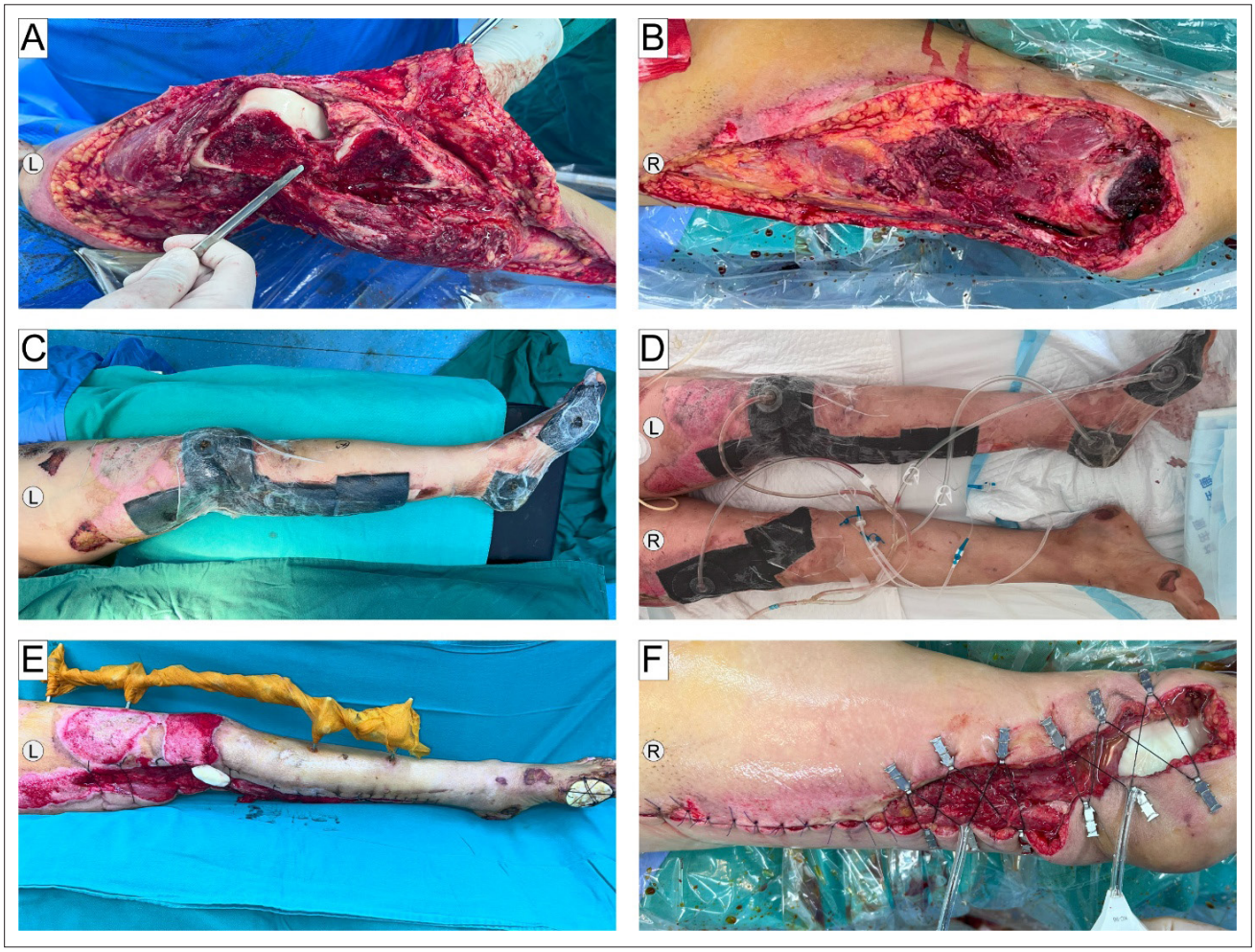

Figure 2. Multiple debridements removing necrotic subcutaneous tissue and contaminated bone, with limb stabilization. (A) Post-debridement exploration of the left knee showing complete loss of the medial femoral condyle and medial tibial plateau, with intact anterior and posterior cruciate ligaments. (B) Partial defect of the medial femoral condyle and absence of the medial collateral ligament on the right knee. (C–D) Wounds covered with VAC® polyurethane foam dressings. (E) Left lower limb stabilized with an external fixation frame following the second debridement. (F) Right lower limb after debridement.

3. Discussion

Periarticular bone and soft tissue defects of the knee caused by high-energy trauma such as traffic accidents, machine crush injuries, and falls from height remain a significant challenge for orthopedic surgeons.[4] The knee joint comprises critical bony structures, including the distal femur, tibial plateau, patella, and proximal tibia, which serve as attachment sites for muscles such as the quadriceps, rectus femoris, and hamstrings. High-energy trauma often results in open fractures and extensive bone and soft tissue loss following emergent debridement, necessitating staged treatment approaches. Conventional management typically involves free flap transfer combined with bone reconstruction techniques such as autologous or allogeneic bone grafting,[5] Masquelet's induced membrane technique,[6] Ilizarov bone transport,[7] and vascularized fibular grafting.[8] However, these approaches often require multiple debridements, prolonged external fixation crossing the knee joint, and are associated with high complication rates, including flap insufficiency, bone exposure, and nonunion. Currently, there is no universally accepted standard treatment for complex bilateral knee defects.

In severe bilateral knee bone defects, patient-specific 3D-printed prostheses offer a promising solution. These implants enable precise anatomical reconstruction with excellent biomechanical properties and biocompatibility.[9] They facilitate accurate anatomic reconstruction, enhanced biomechanical support, and customized integration with surrounding tissues.[10] Recent studies show that 3D-printed

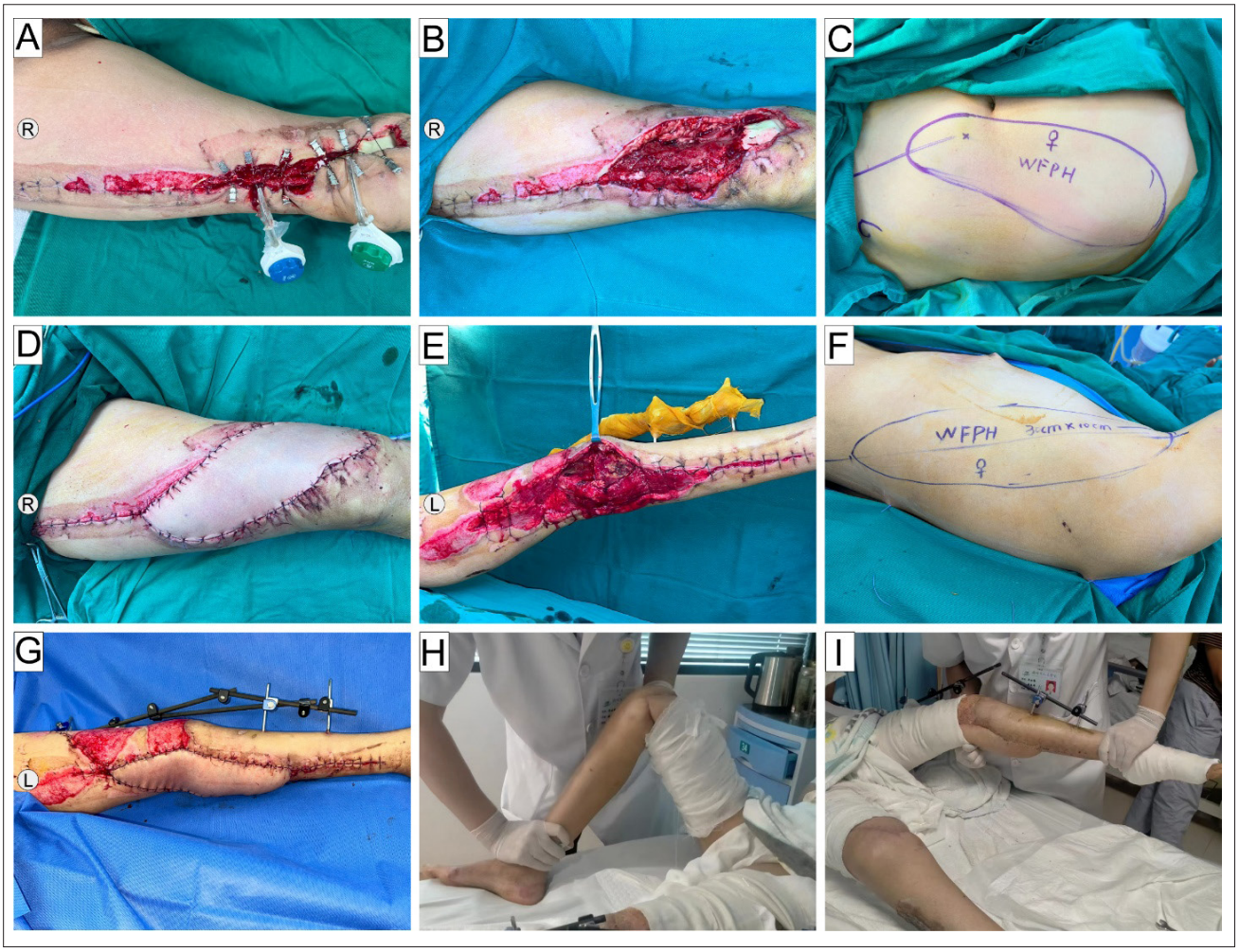

Figure 3. Flap coverage of the wounds. (A, B) Preoperative wound status of the right lower limb. (C) DIEP flap (22 × 14 cm^2) selected for right knee coverage. (D) Revascularization of the right knee DIEP flap. (E) Preoperative wound status of the left lower limb. (F) Latissimus dorsi musculocutaneous flap (30 × 10 cm^2) selected for left knee coverage. (G) Revascularization of the left knee latissimus dorsi flap. (H) Active knee flexion and extension rehabilitation of the right affected limb. (I) Removal of external fixation and initiation of knee flexion and extension rehabilitation of the left affected limb.

titanium prostheses, produced via selective laser sintering, achieve optimal pore size (300–800 μm) and porosity (60–80%), promoting osteoblast migration and vascular ingrowth—effectively overcoming the limitations of traditional grafts in managing large metaphyseal defects.[11] This case highlights a successful staged approach involving radical debridement and early wound coverage, combined with timely functional rehabilitation to prepare for prosthetic implantation. Based on previous research, we designed custom 3D-printed titanium implants using additively manufactured porous scaffolds with a target pore size of 300–400 μm, which are suitable for repairing large segmental bone defects.[12] The design also incorporated tunnels for MCL reconstruction using LARS ligaments, which exhibit excellent biocompatibility, rapid fibroblast ingrowth, and sufficient mechanical tensile strength while minimizing deformation.[13] This integrated approach reflects the growing role of 3D printing in osteochondral-ligamentous reconstruction, enabling simultaneous bone and soft tissue repair. Bilateral MCL reconstruction with LARS provided joint stability and promoted recovery. Postoperative imaging confirmed restored alignment, supporting the feasibility of bilateral 3D-printed knee prostheses for traumatic defects. At 12 months, the patient achieved 120° (left) and 80° (right) knee flexion, Knee Society Scores of 65 and 70, and could walk with small steps, maintaining good quality of life.[14] Mid-term studies report 85–92% 5-year survival rates for 3D-printed implants, affirming their reliability.[15] Patient-specific solutions, like the 3D-printed prosthesis in this

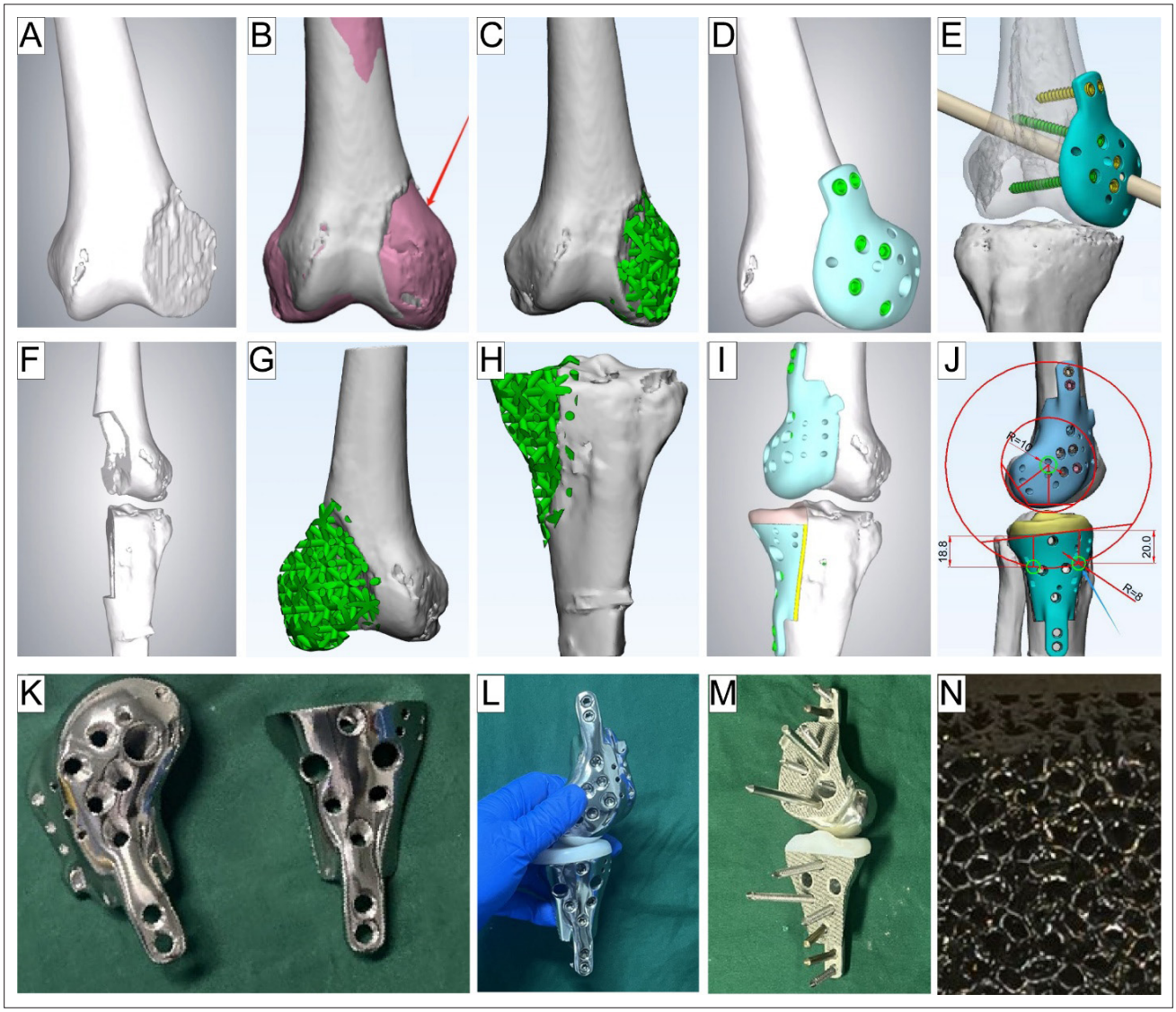

Figure 4. 3D-printed prosthesis design. (A–D) Design of the right medial femoral condyle prosthesis based on data-driven modeling. (E) Confirmation of the prosthesis design including the MCL reconstruction tunnel. (F–I) 3D-printed left knee prosthesis designed by mirroring the reconstructed right knee anatomy. (J) Design of the position and orientation of the MCL (all measurements in the schematic are shown in millimeters). (K, L) External view and assembly method of the left 3D-printed prosthesis. (M) Bone-contacting surface of the left prosthesis. (N) Surface coating of the bone-contacting interface. Abbreviation: MCL, medial collateral ligament.

study, represent a paradigm shift in managing complex joint injuries, but cost-effectiveness needs to be considered in future by adopting standardized designs.

4. Conclusion

The current case demonstrates that when direct mirroring is not feasible for bilateral knee defects, a prosthesis can first be designed for the less affected side using a data-driven approach. After successful implantation, the contralateral prosthesis can then be created by mirroring the reconstructed side. Combined with LARS ligament reconstruction, this staged strategy effectively restored joint stability and function despite extensive bone and ligament loss. It offers a promising solution for complex bilateral knee injuries and may be applicable to other challenging joint reconstructions.

Supplemental information

Video S1. Intraoperative range of motion of the right knee after prosthesis implantation.

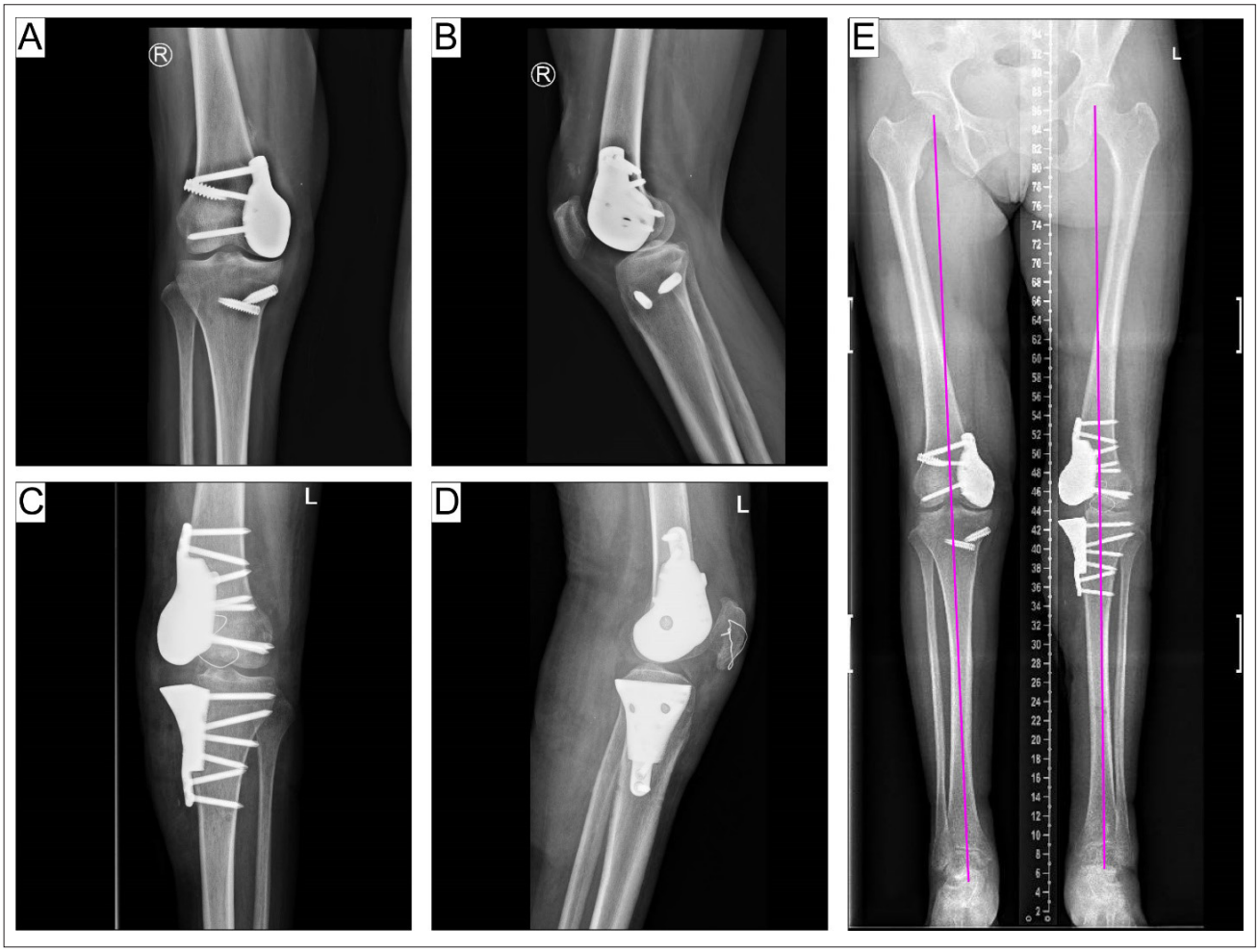

Figure 5. Postoperative radiographs. (A) Anteroposterior radiograph of the right knee post-reconstruction. (B) Lateral radiograph of the right knee post-reconstruction. (C) Anteroposterior radiograph of the left knee post-reconstruction. (D) Lateral radiograph of the left knee post-reconstruction. (E) Full-length lower limb radiograph demonstrating mechanical alignment after bilateral knee reconstructions (lines represent the mechanical axis of both lower limbs).

Video S2. Intraoperative range of motion of the left knee after prosthesis implantation

Video S3. Patient walking condition at 3 months postoperatively.

Video S4. Patient walking condition at 12 months postoperatively.

Acknowledgments

None.

Funding

This work was supported by the National Natural Science Foundation of China (No. 82302031) and the Natural Science Foundation of Shandong Province (No. ZR2024QH033).

Conflict of interest

The authors declare that they have no conflicts of interest.

Author contributions

Conceptualization: Gang Zhao, Xiaoming Yang, Xuecheng Sun, Naibo Feng
Investigation: All authors
Methodology: Gang Zhao, Yongqiang Zhang, Longfei Liu, Futian Zhang, Da Huo, Xiaoming Yang
Writing–original draft: Gang Zhao, Longxin An
Writing–review & editing: Xiaoming Yang, Naibo Feng

Ethics approval and consent to participate

This study was approved by the Ethics Committee of the First Affiliated Hospital of Shandong Second Medical

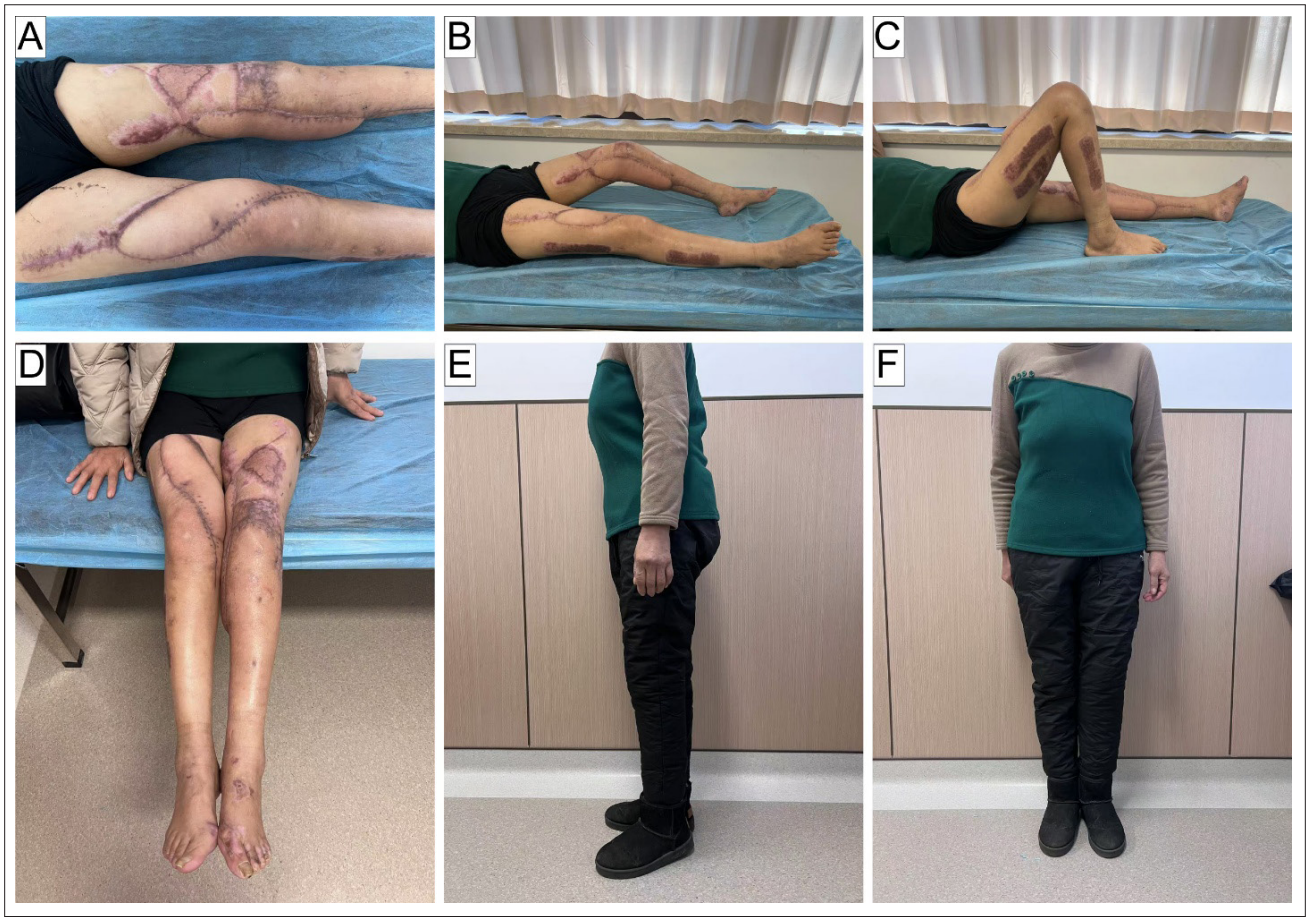

Figure 6. Follow-up. (A) External appearance of both lower limbs at 3 months postoperatively. (B) Active knee flexion of the left leg. (C) Active knee flexion of the right leg. (D) Bilateral lower limb extension. (E) Patient bearing weight normally on both lower limbs at 3 months post-operatively.

University (Approval No. KYLL20250521-7), and informed consent was obtained from the patient.

Consent for publication

Signed consent was obtained from the patient and guardians for the publication of patient-related test results in this paper.

Availability of data

Data will be made available from the corresponding author upon reasonable request.

References

1. Manzotti A, Pullen C, Deromedis B, *et al*. Knee arthrodesis after infected total knee arthroplasty using the Ilizarov method. *Clin Orthop Relat Res*. 2001;(389):143-149. doi: 10.1097/00003086-200108000-00020

2. Oostenbroek HJ, van Roermund PM. Arthrodesis of the knee after an infected arthroplasty using the Ilizarov method. *J Bone Joint Surg Br*. 2001;83(1):50-54. doi: 10.1302/0301-620x.83b1.10572

3. Barwick TW, Montgomery RJ. Knee arthrodesis with lengthening: experience of using Ilizarov techniques to salvage large asymmetric defects following infected peri-articular fractures. *Injury*. 2013;44(8):1043-1048. doi: 10.1016/j.injury.2013.02.017

4. Gupta R, Weisberger J, Herzog I, *et al*. Utilization of the gastrocnemius flap for post-traumatic knee reconstruction: a systematic review. *Eur J Orthop Surg Traumatol*. 2024;34(5):2255-2261. doi: 10.1007/s00590-024-03938-2

5. Azi ML, Aprato A, Santi I, *et al*. Autologous bone graft in the treatment of post-traumatic bone defects: a systematic review and meta-analysis. *BMC Musculoskelet Disord*. 2016;17(1): 465. doi: 10.1186/s12891-016-1312-4

6. Masquelet A, Kanakaris NK, Obert L, *et al*. Bone repair using the masquelet technique. *J Bone Joint Surg Am*. 2019;101(11):1024-1036.
doi: 10.2106/jbjs.18.00842

7. Blázquez-Carmona P, Mora-Macías J, Morgaz J, *et al*. Mechanobiology of bone consolidation during distraction osteogenesis: bone lengthening vs. bone transport. *Ann Biomed Eng*. 2021;49(4): 1209-1221.
doi: 10.1007/s10439-020-02665-z

8. Dheenadhayalan J, Imran A, Devendra A, *et al*. Can locking plate fixation and free vascularised fibular transfer with skin island achieve good functional outcome in the treatment of large bone defects of Tibia ? A study of 26 cases. *Injury*. 2024;55(Suppl 2):111465.
doi: 10.1016/j.injury.2024.111465

9. Meng M, Wang J, Huang H, *et al*. 3D printing metal implants in orthopedic surgery: methods, applications and future prospects. *J Orthop Translat*. 2023;42:94-112.
doi: 10.1016/j.jot.2023.08.004

10. Jing S, Yu A, Dong S, *et al*. 3D-printed prosthesis for traumatic trapezium bone defect: a case report. *Arch Orthop Trauma Surg*. 2025;145(1):182.
doi: 10.1007/s00402-025-05789-w

11. Qu Z, Yue J, Song N, *et al*. Innovations in three-dimensional-printed individualized bone prosthesis materials: revolutionizing orthopedic surgery: a review. *Int J Surg*. 2024;110(10):6748-6762.
doi: 10.1097/js9.0000000000001842

12. Li G, Wang L, Pan W, *et al*. In vitro and in vivo study of additive manufactured porous Ti6Al4V scaffolds for repairing bone defects. *Sci Rep*. 2016;6:34072.
doi: 10.1038/srep34072

13. Core M, Anract P, Raffin J, *et al*. Traumatic patellar tendon rupture repair using synthetic ligament augmentation. *J Knee Surg*. 2020;33(8):804-809.
doi: 10.1055/s-0039-1688564

14. Miralles-Muñoz FA, Gonzalez-Parreño S, Martinez-Mendez D, *et al*. A validated outcome categorization of the knee society score for total knee arthroplasty. *Knee Surg Sports Traumatol Arthrosc*. 2022;30(4):1266-1272.
doi: 10.1007/s00167-021-06563-2

15. Fang S, Wang Y, Xu P, *et al*. Three-dimensional-printed titanium implants for severe acetabular bone defects in revision hip arthroplasty: short- and mid-term results. *Int Orthop*. 2022;46(6):1289-1297.
doi: 10.1007/s00264-022-05390-5